Catalytic Inactivation of Protein Tyrosine Phosphatase CD45 and Protein Tyrosine Phosphatase 1B by Polyaromatic Quinones

Qingping Wang, Daniel Dubé, Richard W. Friesen, Tammy G. LeRiche, Kevin P. Bateman, Laird Trimble, Joe Sanghara, Rebecca Pollex, Chidambaram Ramachandran, Michael J. Gresser, and Zheng Huang*

Department of Biochemistry and Molecular Biology, Merck Frosst Centre for Therapeutic Research, Post Office Box 1005, Pointe Claire, Dorval, Quebec H9R 4P8, Canada

Received November 6, 2003; Revised Manuscript Received February 2, 2004

ABSTRACT: Polyaromatic quinones, such as the environmental pollutants 9,10-phenanthrenediones, elicit a wide range of responses including growth inhibition, immune suppression, and glucose normalization in diabetic models. Yet the molecular mechanisms behind these effects remain controversial. Here we report that many of them are oxygen-dependent and catalytic inactivators of protein tyrosine phosphatases (PTP). Under aerobic conditions, the PTP inactivation by 2-nitro-9,10-phenanthrenedione followed a pseudo-first-order process, with the rate of inactivation increasing nearly linearly with increasing inhibitor concentration, yielding apparent inactivation rate constants of 4300, 387, and 5200 M^{-1} s^{-1} at pH 7.2 against CD45, PTP1B, and LAR, respectively. The rate of CD45 inactivation increased ∼25-fold from pH 6.0 to 7.5, with complete inactivation achieved using a catalytic amount (0.05 molar equiv) of the inhibitor. The quinone-catalyzed CD45 inactivation was prevented by catalase or superoxide dismutase. Inactivated CD45 after ^{125}I-9,10-phenanthrenedione treatment carried no radioactivity, indicating the absence of a stable inhibitor/enzyme complex. The activity of inactivated CD45 was partially restored (∼10%) by hydroxylamine or dithiothreitol, supporting the presence of a small population of sulfenic acid or sulfenyl-amide species. Treatment of PTP1B with 2-nitro-9,10-phenanthrenedione resulted in the specific and sequential oxidation of the catalytic cysteine to the sulfinic and sulfonic acid. These results suggest that reactive oxygen species and the semiquinone radical, continuously generated during quinone-catalyzed redox cycling, mediate the specific catalytic cysteine oxidation. Naturally occurring quinones may act as efficient regulators of protein tyrosine phosphorylation in biological systems. Aberrant phosphotyrosine homeostasis resulting from continued polyaromatic hydrocarbon quinone exposure may play a significant role in their disease etiology.

Polyaromatic *o*- and *p*-quinones (1,2- and 1,4-quinones) are oxidative metabolites of catechols, catecholamines, and the ubiquitous environmental pollutants polyaromatic hydrocarbons (PAH)[1] derived from incomplete combustion of fossil fuels and tobacco smoking (*1*, *2*). The majority of quinones are highly bioactive compounds. Some are mutagenic while others are immunosuppressive (*3*−*4*). Several quinoids selectively induce apoptosis of cancer cells, and they are used clinically as chemotherapeutic agents (*5*, *6*). Despite their potent biological activities, the mechanism of action for many of the bioactive quinones remains controversial. Two closely related chemical properties are thought to be responsible for their physiological and toxicological properties. First, their electrophilicity leaves them susceptible to nucleophilic attack, resulting in the covalent modification of protein nucleophiles. Second, they undergo redox cycling, in the presence of oxygen and tissue-reducing equivalents, such as glutathione, ascorbate, and NAD(P)H, to produce and accumulate reactive oxygen species including hydrogen peroxide (H_2O_2), superoxide anion radical ($O_2^{-\bullet}$), and semiquinone anion radical ($SQ^{-\bullet}$), which cause DNA and protein damage (*7*−*10*).

The reversible protein tyrosine phosphorylation by the opposing activities of protein tyrosine kinases (PTK) and protein tyrosine phosphatases (PTP) is a key element of the signaling pathways induced by environmental stimuli that regulates a wide range of cellular processes (*11*, *12*). Increasing evidence suggests that the cellular redox state regulates PTP activity through the reversible oxidation of the catalytic cysteine to the sulfenic acid (Cys−SOH) or the sulfenyl-amide intermediate (*13*−*17*). Aberrant phosphotyrosine levels from the imbalance of PTK and PTP activities have been implicated in the development of a number of diseases including cancer, diabetes, and obesity (*18*). CD45

* To whom correspondence should be addressed: fax (514) 428-4900; tel (514) 428-3143; e-mail zheng_huang@merck.com.

[1] Abbreviations: AhR, aryl hydrocarbon receptor/transcription factor; Bis-Tris, bis(2-hydroxyethyl)aminotris(hydroxymethyl)methane; BSA, bovine serum albumin; CD45, leukocyte phosphatase (leukocyte common antigen); DMF, dimethylformamide; DMH, *N*,*N*′-dimethyl-*N*,*N*′-bis(mercaptoacetyl)hydrazine; DMSO, dimethyl sulfoxide; DTT, dithiothreitol; EDTA, ethylenediaminetetraacetic acid; FDP, 3,6-fluorescein diphosphate; FMP, fluorescein monophosphate; HEPES, *N*-(2-hydroxyethyl)piperazine-*N*′-2-ethanesulfonic acid; LAR, leukocyte common antigen-related protein; (HP)LC, (high-performance) liquid chromatography; MS and MS/MS, regular and tandem mass spectroscopy; MUP, 4-methyl-7-hydroxycoumarinyl phosphate; NAD(P)H, nicotinamide adenine dinucleotide (phosphate), reduced form; NBDCl, 7-chloro-4-nitrobenzo-2-oxa-1,3-diazole; $O_2^{-\bullet}$, superoxide anion radical; PAH, polycyclic aromatic hydrocarbons; PTK, protein tyrosine kinase; PTP, protein tyrosine phosphatase; ROS, reactive oxygen species; SOD, superoxide dismutase; $SQ^{-\bullet}$, semiquinone anion radical; TFA, trifluoroacetic acid; Tris, tris(hydroxymethyl)aminomethane.

10.1021/bi035986e CCC: $27.50
Published on Web 03/19/2004

plays an essential role in T-cell receptor-coupled signaling processes (*19*). PTP1B is the negative regulator of insulin receptor signaling. Mice lacking functional PTP1B exhibit increased sensitivity toward insulin and are resistant to obesity (*20*). Selective inhibition of CD45 and PTP1B may offer new opportunities for therapeutic intervention in various autoimmune diseases, type II diabetes mellitus, and obesity.

PTPs share a conserved active site with an invariant Cys residue as the catalytic nucleophile. Surrounding the thiolate anion are positively charged amino acids (arginines and lysines) that interact with the negatively charged phosphate of the substrate. In addition, several hydrophobic interactions with the phenyl of the phosphotyrosine contribute to their preference for phosphotyrosine substrates. Catalysis involves the formation of a thiophosphate enzyme intermediate, which is hydrolyzed in a second step(*11*). These features of the catalytic machinery have led to the identification of more effective alternative substrates and several classes of reversible inhibitors. On the other hand, these properties also render the catalytic cysteine particularly sensitive to aromatic electrophiles and oxidizing agents, forming covalent adducts with α-haloacetophenone and Michael acceptors and forming oxidized cysteine with hydrogen peroxide, superoxide anion radical, peroxynitrite, pervanadate, and alendronate. The properties of many of these inhibitors, including their modes of action, have recently been summarized in a comprehensive review (*21*).

The search for protein tyrosine phosphatase inhibitors of CD45, PTP1B, and Cdc25 has led to the identification and optimization of a number of quinones, which share the nucleus of 9,10-phenanthrenedione and 1,2- and 1,4-naphthoquinone (*22*−*30*). In addition to suppressing receptor-mediated cell proliferation, several of these quinones are efficacious in normalizing the glucose levels of diabetic animals (*22*, *24*). However, the molecular mechanism of their PTP inhibition remains controversial. We had independently identified 9,10-phenanthrenedione derivatives as potent and nonselective PTP inhibitors from screening Merck's sample collection (*31*). With the use of radiolabeled inhibitor and mass spectrometric analysis, herein we report that 9,10-phenanthrenedione-mediated CD45 and PTP1B inhibition is an oxygen-dependent and catalytic process, resulting in the specific oxidation of the catalytic cysteine.

MATERIALS AND METHODS

General Procedures. Fluorescence spectra were recorded on a LS-50 B spectrophotometer (Perkin-Elmer) equipped with four stirred quartz cuvettes or on a 96-well fluorescence plate reader (Spectra-Max Gemini, Molecular Devices). ^{1}H NMR spectra were recorded at 300 MHz in acetone-d_6. Broadband-decoupled ^{13}C NMR spectra were recorded at 125 MHz in acetone-d_6 with solvent as the internal standard. IR spectra were recorded on solutions in $CHCl_3$. Workup procedures involving the drying of organics were done with $MgSO_4$. Column chromatography was carried out on 230−400 mesh silica gel (40−63 μm), eluting with the solvents indicated. Elemental analyses were performed by Oneida Research Services, Inc., Whitesboro, NY.

MS and MS/MS data were acquired on a Micromass Q-ToF Ultima mass spectrometer (Manchester, U.K.) fitted with a Z-spray electrospray ion source. The mass spectrometer was operated in positive-ion mode at a capillary voltage of 3.5 kV with desolvation gas and source temperatures of 150 and 80 °C, respectively. The tunnel voltage was maintained at 50 V while the collision voltage (for MS/MS experiments) was adjusted according to the mass of the parent peptide (25−35 V). Samples were delivered to the mass spectrometer by an Agilent 1100 capillary-LC (Palo Alto, CA). Protein analysis was carried out at a flow rate of 50 μL/min on a ThermoHypersil 50 × 1 mm BioBasic-4 5 μm column. A linear gradient was run from 15% to 95% B over 20 min. Eluent A was 5% CH_3CN/0.05% TFA, and eluent B was 50% CH_3CN/50% 2-propanol/0.05% TFA. The tryptic digestion of PTP1B was performed on a Phenomenex 150 × 1 mm C18 (3 μm) Luna column. Eluent A consisted of 5% CH_3CN/0.1% formic acid, while eluent B was 95% CH_3CN/0.1% formic acid; a gradient was used that started at 5% B and increased linearly to 60% B over 30 min at a flow rate of 20 μL/min.

Reagents. Catalase from bovine liver (2000∼5000 units/mg), superoxide dismutase from horseradish (1000∼4000 units/mg), and buffers were from Sigma Chemical Co (St. Louis, MO). NBDCl (7-chloro-4-nitrobenzo-2-oxa-1,3-diazole) was from Molecular Probes (Eugen, Oregon). Quinones and diketones except 2-iodo-9,10-phenanthrenedione were from Aldrich or the Sigma−Aldrich Library of Rare Chemicals (Milwaukee, WI). 2-Iodo-9,10-phenanthrenedione and 2-[^{125}I]-9,10-phenanthrenedione were prepared as detailed below. 3,6-Fluorescein diphosphate (FDP) and *N*,*N*′-dimethyl-*N*,*N*′-bis(mercaptoacetyl)hydrazine (DMH) were synthesized in house.

2-Iodo-9,10-phenanthrenedione. The compound was prepared by a modification of the reported procedure (*32*). To a mixture of commercially available phenanthrenequinone (416 mg, 2 mmol) and iodine (761 mg, 3 mmol) in glacial acetic acid (8 mL) and concentrated H_2SO_4 (0.5 mL) at 100 °C was added HNO_3 (0.2 mL). The resulting mixture was stirred for 4 h and then cooled to room temperature. Water (25 mL) was added and the resulting solid was collected by filtration and washed successively with water, 10% $Na_2S_2O_3$, and water. The residual solid was purified by flash chromatography (15:1 toluene/ethyl acetate, v/v). The title compound (350 mg, 22%) was obtained as a bright orange solid, mp 232−235 °C (lit. 225 °C). IR 1680 cm^{-1}; ^{1}H NMR δ 7.59 (ddd, 1H, J = 1.1, 7.4, 7.8 Hz), 7.82 (ddd, 1H, J = 1.5, 7.4, 8.0 Hz), 8.10 (br d, 1H, J = 8.5 Hz), 8.11 (ddd, 1H, J = 0.5, 1.5, 7.8 Hz), 8.16 (dd, 1H, J = 1.9, 8.5 Hz), 8.29 (dm, 1H, J = 8.0 Hz), 8.37 (dd, 1H, J = 0.4, 1.9 Hz); ^{13}C NMR (125 MHz, acetone-d_6) δ 95.2, 125.3, 127.3, 130.5, 130.7, 132.5, 133.7, 136.0, 136.2, 136.6, 138.8, 144.9, 179.4, 179.6; exact mass calcd for $C_{14}H_8IO_2$ $(M + H)^+$ 334.9569, found 334.9569. Anal. calcd for $C_{14}H_7IO_2$: C, 50.33; H, 2.11. Found: C, 49.73; H, 2.07.

2-Trimethylstannylphenanthrenequinone. A mixture of 2-iodophenanthrenequinone (49 mg, 0.15 mmol), hexamethylditin (0.14 mL, 0.45 mmol), and $Pd(Ph_3P)_4$ (20 mg, 0.015 mmol) in 1,4-dioxane (10 mL) was refluxed for 5 min. The mixture was concentrated in vacuo and the residue was subjected to flash chromatography (3:1 hexane/ethyl acetate, v/v). The title compound (30 mg, 56%) was obtained as a yellow solid, mp 177−180 °C. IR 1680, 1295, 1285 cm^{-1}; ^{1}H NMR δ 0.38 (s, 9H, J_{Sn-H} = 56 Hz), 7.54 (dt, 1H, J = 1.0, 7.6 Hz), 7.80 (ddd, 1H, J = 1.5, 7.4, 8.0 Hz), 7.95 (dd,

1H, $J = 1.2$, 7.8 Hz, $J_{Sn-H} = 39$ Hz), 8.09 (dd, 1H, $J = 1.2$, 7.7 Hz), 8.16−8.30 (m, 3H); exact mass calcd for $C_{17}H_{17}O_2Sn$ $(M + H)^+$ 373.0251, found 373.0250. Anal. calcd for $C_{17}H_{16}O_2Sn$: C, 55.03; H, 4.35. Found: C, 54.28; H, 4.35.

2-[^{125}I]-9,10-Phenanthrenedione. A reaction vial was charged with 2-trimethylstannylphenanthrenequinone (80 μL of a 1.5 mg/250 μL solution in MeCN, 4 μmol), MeOH (200 μL), Na^{125}I (40 μL of an aqueous solution of 5 mCi/100 μL), and chloramine-T hydrate (20 μL of a 15 mg/mL solution in pH 7 phosphate buffer). After 30 min at room temperature, saturated aqueous $Na_2S_2O_3$ (20 μL) and DMF (100 μL) were added successively. The crude mixture was purified by HPLC (Waters RCM C-18 cartridge (2.5 × 1.0 cm); mobile phase was 66% MeOH/33% water, with UV analysis at 265 nm; retention time 9.1 min). The title compound (525 μCi) was contained in 4 mL of eluant.

^{18}O/^{16}O Exchange of 2-Iodo-9,10-phenanthrenedione by ^{13}C NMR. Oxygen exchange on both carbonyls of 2-iodo-9,10-phenanthrenedione with ^{18}O-water was monitored by use of the characteristic ^{18}O-induced upfield shift of their ^{13}C NMR signal according to the published procedure (*33*). Briefly, 2-iodo-9,10-phenanthrenedione (10 mg) was dissolved in a mixed solvent containing deuterated THF/H_2O (v/v 9:1 with 20% $H_2{}^{18}O$). ^{13}C NMR chemical shifts of the carbonyl carbons were assigned at 178.93 ppm for C_9 and 178.72 ppm for C_{10} from ^{1}H−^{1}H and ^{1}H−^{13}C correlation spectra. Two upfield-shifted peaks, at 178.88 ppm for C_9 and 178.67 ppm for C_{10}, corresponding to the ^{18}O labeled carbonyls, emerged rapidly within the duration of the experiment (∼30 min) with their intensities comparable to the 20% equilibrium value.

Recombinant PTPs. The catalytic domains of recombinant human CD45, PTP1B, and LAR were expressed and purified to homogeneity according to the procedure previously described (*34*, *35*). Protein concentrations were estimated with the protein assay kit from Bio-Rad with BSA as protein standard.

PTP Activity Assay. PTP activity was monitored continuously with FDP as substrate according to the published procedure (*34*). Typically, the assay buffer (200 μL) contained 20 mM HEPES (pH 7.0), 100 mM NaCl, 1 mM EDTA, 1 mM DTT. Bis-Tris (50 mM) and Tris (50 mM) were used in place of HEPES at pH 6 and pH 7.5. A subsaturating concentration of FDP (20 μM) was used to monitor the PTP activity unless otherwise specified. The formation of product FMP from FDP was monitored continuously by fluorescence at 515 nm with excitation at 460 nm. Inhibitors were introduced via 2 μL of DMSO, and the 1% (v/v) final concentration of DMSO exerted a negligible effect on enzyme activity. The reaction was typically initiated by the addition of 30−50 ng of PTP to the assay buffer containing substrate and inhibitor. Oxygen-free buffer was prepared by two freeze/thaw cycles under high vacuum and exchanged under argon. The reaction mixture was prepared by charging a rubber septum-sealed Eppendorf tube with 200 μL of the oxygen-depleted buffer, 10 μL of CD45 (11 μg, final concentration ∼7 μM), and 2 μL of 2-nitro-9,10-phenanthrenedione in DMSO (final concentration 0.35 and 0.7 μM) under argon. Aliquot (10 μL) time points were diluted into 2 mL of assay buffer and monitored for residual activity within the first 5 min.

CD45 Inactivation by 2-[^{125}I]-9,10-Phenanthrenedione. 2-[^{125}I]-9,10-phenanthrenequinone (1.5 μM, 0.5 equiv, radioactivity ∼ 100 000 dpm) was incubated with (or without) 3 μM CD45 for 6 h at room temperature in 50 μL of buffer containing 20 mM HEPES (pH 7.2), 1 mM EDTA, and 1 mM DTT. Over 95% of the enzyme activity was lost after the incubation. The inactivated CD45 was separated from the unbound inhibitor by filtering through a Centricon-10 filtration unit (Amicon, Inc.) according to the manufacturer's instructions. The inactivated CD45, retained on the membrane, was washed three times with 1 mL of the incubation buffer to remove the residual unbound inhibitor. Radioactivity on the membrane and in the filtrate were determined on a LS-6000 scintillation counter (Beckman Instrument Inc. CA).

Reactivation by Hydroxylamine. CD45 (0.5 μM) in 100 μL of buffer (20 mM HEPES at pH 7.2, 1 mM EDTA, and 1 mM DTT) was incubated with (a) 10 μM 2-iodo-9,10-phenanthrenedione (via 2 μL of DMSO) and (b) 2 μL of DMSO. After 30 min at room temperature, the reaction mixture (10 μL) was diluted with 1.5 mL of assay buffer containing 20 mM (or 0 mM) hydroxylamine, 20 μM FDP, 1 mM EDTA, 1 mM DTT, 0.01% BSA (w/v), and 100 mM HEPES (pH 7.2) to monitor the residual activity. Enzyme activity at any given time was determined from the first-order derivative of fluorescence vs time. The half-life of the reactivation process was determined by fitting the velocity vs time to a first-order rate equation. The final steady-state velocity was compared with the initial rate of CD45 in the absence of inhibitor to calculate the percentage of activity recovery.

Labeling with 7-Chloro-4-nitrobenzo-2-oxa-1,3-diazole. Labeling of PTP1B by NBDCl was carried out following the published procedure (*36*). Briefly, PTP1B (10 μM) was incubated, at room temperature, in a final volume of 200 μL of buffer [50 mM Bis-Tris (pH 6.5), 1 mM EDTA, and 1 mM DTT] with (a) DMSO (5 μL), (b) 10 μM 2-nitro-9,10-phenanthrenedione (via 5 μL of DMSO), or (c) 10 μM 2-nitro-9,10-phenanthrenedione (via 5 μL of DMSO) plus 100 μM Glu-F_2PMP−F_2PMP, a competitive inhibitor of PTP1B with a K_i ∼ 40 nM (*37*). After >90% PTP activity was inhibited for sample b, the unbound inhibitors were removed by dialysis under argon. NBDCl (0.8 mM) was added to each of the resulting solutions and incubated for 90 min at room temperature. Excess NBDCl was removed from the labeled PTP1B by passing through a Centri-Spin filtration column (Princeton Separation, Princeton, NJ) before spectrum measurement.

Mass Spectrometric Analysis. PTP1B (2.4 μM) was incubated with 0 or 2.5 μM 2-nitro-9,10-phenanthrenedione at 0 °C under air in a 100 μL buffer containing 50 mM Bis-Tris (pH 6.3), 1 mM EDTA, and 1 mM DTT. Aliquots were analyzed for residual activity and protein modification by mass spectrometry after 0, 2, 4, and 5 h of incubation. The modified PTP1B after 5 h of incubation (<10% activity remained) was passed through a Centri-Spin column to remove unbound inhibitor. The control sample was processed in parallel. The samples, after adjusting to pH 8.5 with NaOH, were incubated overnight at 37 °C with sequence-grade trypsin (1:10 w/w). Following digestion, the peptides were concentrated on the C_{18}-Ziptip, prerinsed sequentially with 75% MeOH/0.05% formic acid and 0.05% formic acid

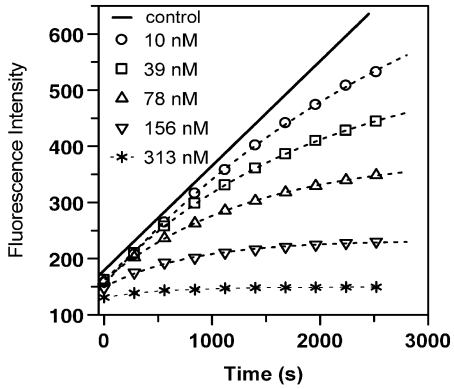

FIGURE 1: Time-dependent inhibition of CD45 by 2-nitro-9,10-phenanthrenedione under air at room temperature. Increased concentrations of inhibitor were mixed with FDP-containing assay buffer and the hydrolysis of FDP to FMP was initiated by the addition of CD45 (see Materials and Methods for details). The time course of CD45-mediated hydrolysis in DMSO alone is displayed as a solid line. The progress curves were fitted by use of a first-order equation to determine the observed inactivation rate constant (k_{obs}).

in water. Approximately 75 μL of the sample was applied repeatedly to the tip. Salts were removed by the application of 250 μL of 0.05% formic acid while the peptides were eluted in 15 μL of 75% MeOH/0.05% formic acid. The peptides were then dried down and reconstituted in 12 μL of 0.05% formic acid for analysis.

Data Analysis. Data were analyzed by the nonlinear iterative regression routine in Grafit (Erithacus Software) and expressed as mean ± SE of ≥3 independent experiments unless otherwise specified. The time-dependent reaction progress curve was approximated by a first-order equation. The resulting inactivation rate increased nearly linearly with increasing inhibitor concentration after an initial lag phase. The slope of the linear response region, indexed as the apparent inactivation rate constant, was used to rank the potency of inhibitors.

RESULTS

Time-Dependent Irreversible Inactivation of CD45 by 2-Nitro-9,10-phenanthrenedione. Under aerobic conditions and in the presence of 1 mM DTT, 2-nitro-9,10-phenanthrenedione potently inhibited CD45 in a time- and dose-dependent manner as shown in Figure 1. The activity of CD45, monitored continuously following the production of FMP from FDP, decreased in a pseudo-first-order process. The observed rate of inactivation increased nearly linearly with increased inhibitor concentration, yielding an apparent inactivation rate constant of 4300 ± 400 M^{-1} s^{-1} at pH 7.2 within the linear response zone (Figure 2). Higher quinone concentrations led to an accelerated rate of enzyme inactivation, which was too rapid to be quantified accurately in a stirred cuvette. In the presence of 2 μM quinone, the half-life of inactivation was 1.4 min, and the inhibition was not reversed by volume dilution with assay buffer. To evaluate the thiol requirement and circumvent the rapid loss of enzyme activity in its absence (CD45 had a half-life < 2 min when DTT was <10 nM under aerobic conditions), the DTT concentration was reduced from 1 mM to ~50 nM. Under these conditions, the spontaneous loss of CD45 activity had a variable half-life from 8 to 10 min, and the presence of 2 μM quinone only slightly perturbed the loss of activity with

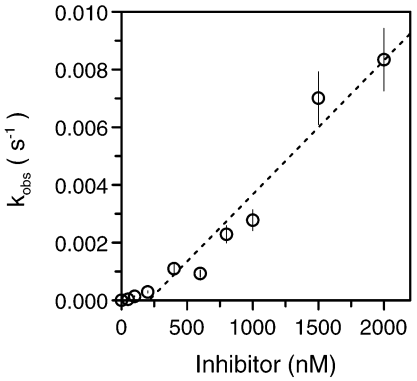

FIGURE 2: Observed inactivation rate (k_{obs}) of CD45 (n = 3) as a function of 2-nitro-9,10-phenanthrenedione concentration under air. After an initial lag phase (<200 nM), the dose−response is near linear with increased inhibitor concentration with a slope at 4300 (±400) M^{-1} s^{-1}.

Table 1: CD45 Inhibition by *o*- and *p*-Quinones and 1,2-Diones under Air[a]

Structure	$k_{inactivation}$ ($M^{-1}s^{-1}$)	Compound
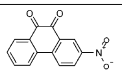	4300 ± 400	2-nitro-9,10-phenanthrenedione
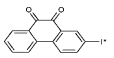	2000 ± 250	2-iodo-9,10-phenanthrenedione
	1030 ± 150	9,10-phenanthrenedione
	420 ± 50	1,2-naphthoquinone
	21 ± 11	1,4-naphthoquinone
	0% In @ 5 μM	S91467-5
	~ 5% In @ 10 μM	Phenylglyoxal
	~ 5 % In @ 10 μM	Phenylpropyldione
	0% In @ 50 μM	1,2-cyclohexanedione

[a] $k_{inactivation}$ (mean ± SE, n ≥ 3) were obtained in 20 mM HEPES (pH 7.2), 1 mM DTT, 1 mM EDTA, and 100 mM NaCl at room temperature. Quinones, except the inactive S91467-5, all exhibited time-dependent inhibition of CD45. The apparent inactivation rate constant is calculated from the linear slope of the dose−response curve. The percentage of inhibition (% In) listed was after 30 min of compound incubation.

the apparent half-life remaining at 5−8 min (n = 3). Thus, the reduced DTT concentration significantly reduced the quinone-mediated rapid CD45 inactivation observed at 1 mM DTT under aerobic conditions.

Structure-Dependent Inactivation. In addition to 2-nitro-9,10-phenanthrenedione, its close structural analogues, 2-iodo-9,10-phenanthrenedione, 9,10-phenanthrenedione, and 1,2- and 1,4-naphthoquinones, inactivated CD45 with apparent inactivation rate constants of 2000, 1030, 420, and 21 M^{-1} s^{-1}, respectively, at pH 7.2 (Table 1). Similar to the case with 2-nitro-9,10-phenanthrenedione, these inhibitors all exhibited a near-linear dose−response in their pseudo-first-order inactivation rate with respect to increased inhibitor concentration up to 10 μM. On the other hand, S91467-5

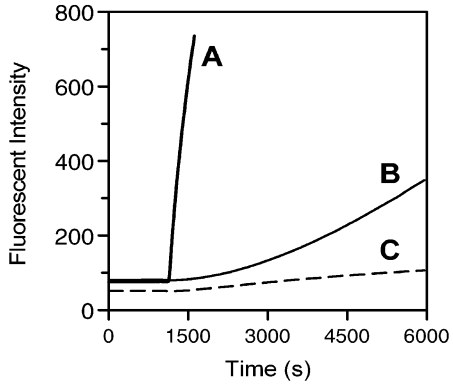

FIGURE 3: Reactivation time course of 2-nitro-9,10-phenanthrenedione-inhibited CD45 by hydroxylamine under air. CD45 (A) and inactivated CD45 (B, C) were diluted ~150-fold into an assay buffer containing 0.01% (w/v) BSA in the presence (B) or absence (C) of 20 mM hydroxylamine. The carried-over inhibitor (~66 nM) had a negligible effect on the time course in the presence of BSA. The activities of CD45 (1.5 intensity units/s) were identical in the presence or absence of hydroxylamine. In the absence of hydroxylamine (C), the inactivated CD45 had a residual rate of 0.01 intensity unit/s (0.6% of control) from incomplete inactivation. In the presence of hydroxylamine (B), the activity of the inactivated CD45 recovered in a first-order process with a half-life of 40 min. Its final steady-state rate was 0.16 intensity unit/s (~10% of control).

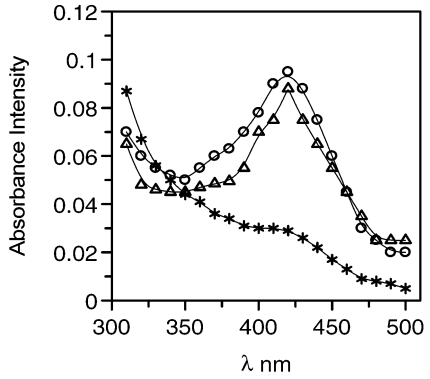

FIGURE 4: Absorption spectra of the covalently labeled PTP1B by NBDCl. PTP1B (10 μM) was incubated for 5 h at room temperature with DMSO (○), 10 μM 2-nitro-9,10-phenanthrenedione (*), and 10 μM 2-nitro-9,10-phenanthrenedione plus 100 μM Glu-F_2PMP−F_2PMP (△). After removal of inhibitors through dialysis under argon, the resulting solutions were treated with 0.8 mM NBDCl for 90 min. UV spectra were recorded after removal of the excess NBDCl. Close to stoichiometric labeling was detected for PTP1B (○) and PTP1B protected by the competing inhibitor (△) based on the extinction coefficient of 13 000 M^{-1} cm^{-1} for the thiol−NBD adduct (*34*).

(Aldrich, Table 1), a close analogue sharing the aromatic 1,2-dione functionality, was inactive. Other 1,2-dione containing compounds, phenylglyoxal, phenylpropyldione and cyclohexanedione, known for their reactivity toward arginine residues, including those in PTPs (*38*, *39*), exerted ≤5% inhibition at 10 μM when they were incubated up to 30 min under the assay conditions. The addition of 0.1 mM arginine had no detectable effect on the rate of CD45 inactivation by 2-nitro-9,10-phenenthrenedione. Hence the bimolecular reaction of the inhibitor with arginine was negligible in comparison with its rapid inactivation of CD45, despite the arginine concentration being >3 log units higher than that of CD45 (~20 nM). In addition to CD45, 2-nitro-9,10-phenanthrenedione also potently inhibited PTP1B and LAR with apparent inactivation rate constants of 387(±50) and 5200 (±500) M^{-1} s^{-1} respectively. Similar to that observed for CD45, the pseudo-first-order inactivation rate of the inhibitor on PTP1B and LAR increased nearly linearly with increased inhibitor concentrations up to 10 μM.

Partial Reactivation by Hydroxylamine or DTT. The pseudo-first-order inactivation rate of CD45 by 200 nM 2-nitro-9,10-phenanthrenedione, monitored by FDP hydrolysis, was reduced by ~50% in the presence of 1 mM MUP, a competing substrate near its K_m (1.1 mM) under the assay conditions (*35*), supporting the postulate that the inhibition was active-site-directed. Contrary to the lack of reactivation by dilution, the activity of the inactivated CD45 was partially restored by nucleophilic reducing agents such as hydroxylamine (Figure 3). The activity of CD45 was not affected by the presence or absence of hydroxylamine and is represented by curve A. The inactivated CD45, after treatment with 10 μM 2-nitro-9,10-phenanthrenedione for 30 min, was time-dependently reactivated after dilution (~150-fold) into an assay buffer containing 20 mM hydroxylamine and 0.01% (w/v) BSA, as signified by the upward curvature in curve B. The presence of BSA in the assay buffer significantly reduced the effect of the carried-over inhibitor to a negligible level, likely by reducing its free concentration. The reactivation followed a first-order process with a half-life of ~40 min. By comparing its final steady-state rate in curve B with the initial activity of CD45 in curve A, ~10% of total activity was recovered. In the absence of hydroxylamine, minimal reactivation was detected, as evidenced by the lack of an upward curvature (linear instead) in curve C. Its residual activity, at ~0.6% of the total activity, was mainly from the incomplete inactivation of CD45. Two thiol-containing nucleophilic reducing agents, DTT (20 mM) and DMH (20 mM), also reactivated the inhibited enzyme to a similar extent (data not shown). These results suggested that a small population of the inactivated enzyme existed either as a diketone/arginine adduct or in the sulfenic acid, sulfenyl-amide, or disulfide states. All these putative species are known to be sensitive to nucleophilic reducing agents, which could potentially mediate reactivation (*16*, *17*, *38*−*41*).

Modification of the Catalytic Cysteine. Earlier studies indicate that the active-site thiol of PTP1B forms a stable thiolate−NBD adduct with a characteristic absorption near 420 nm as illustrated in Figure 4 (○) (*13*, *36*). In contrast, PTP1B preinactivated by 2-nitro-9,10-phenanthrenedione lacks the ability to form the thiol−NBD adduct (*). The addition of 100 μM Glu-F_2PMP−F_2PMP, an active-site-directed reversible inhibitor of PTP1B with a K_i of 40 nM (*37*), completely shielded the active-site thiol from the 2-nitro-9,10-phenanthrenedione-mediated modification. Quantitative formation of the thiol−NBD adduct was detected after the removal of both inhibitors through dialysis (△). We were unable to detect the presence of the putative sulfenic acid−NBD adduct in PTP1B treated with 2-nitro-9,10-phenanthrenedione either by mass spectral analysis or from its characteristic absorption near 347 nm (*13*). This could be due to its low abundance inferred from the limited reactivation (~10%) by hydroxylamine.

Absence of a Radiolabeled Inhibitor/CD45 Complex. The ketone functionality and other electrophilic centers of quinones render them susceptible to nucleophilic additions by protein nucleophiles, including the guanidinium group of

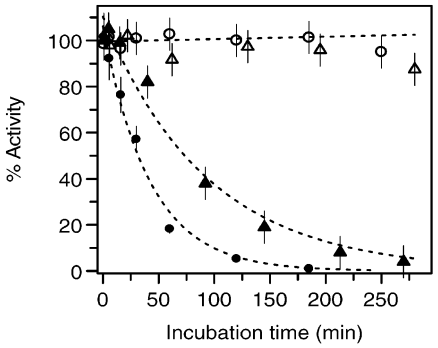

FIGURE 5: Oxygen-dependent catalytic inactivation of CD45 by 2-nitro-9,10-phenanthrenedione. CD45 (7 μM) was incubated with 0.35 μM (0.05 equiv) or 0.7 μM (0.1 equiv) of 2-nitro-9,10-phenanthrenedione in air or under argon at room temperature. The residual CD45 activity was determined by diluting the reaction mixture into FDP-containing buffer. In the absence of inhibitor, CD45 activity was stable in air (○) or under argon (data not shown) up to 5 h under the conditions. Under argon, minimal inhibitions were detected for 0.35 μM (△) or 0.7 μM inhibitor (data not shown). In air, the enzyme activity decayed exponentially with a half-life of 64 min at 0.35 μM (▲) and a half-life of 30 min at 0.7 μM (●) inhibitor.

arginine, the amine of lysine, and the thiol of cysteine, to form various stable covalent adducts in solution (*8*, *10*). The 1,2-diketone/arginine adduct remains sensitive to hydroxylamine-mediated hydrolysis (*38*). To evaluate the involvement of these protein adducts in mediating the inactivation of CD45, radiolabeled 2-[^{125}I]-9,10-phenanthrenedione was prepared (see Materials and Methods for details). After >95% of CD45 (3 μM) activity was inhibited by 1.5 μM (0.5 equiv) of the radiolabeled inhibitor, the resulting inactivated CD45 was separated from the rest of the incubation mixture by filtration through a membrane filter. Of the total radioactivity, 75% ± 4% ($n = 3$) was recovered in the filtrate with the rest remained on the membrane. Parallel samples without CD45 had a comparable radioactivity distribution with 83% ± 3% ($n = 3$) in the filtrate. The result suggested that most of the membrane-bound radioactivity was from nonspecific binding. Therefore, the inactivated CD45 carried ~8% ± 4% of total radioactivity, which translated to 0.04 (±0.02) equiv of radioactivity based on a stoichiometric inhibitor/CD45 ratio. This result eliminated the formation of a stable CD45−inhibitor complex as the reason for inhibition. Interestingly, the unbound radioactivity recovered in the filtrate comigrated with authentic 2-[^{125}I]-9,10-phenanthrenedione on a reverse-phase (C_{18}) HPLC column, raising the possibility that the inhibitor was regenerated during incubation.

Oxygen-Dependent and Catalytic Inactivation of CD45 by 2-Nitro-9,10-phenanthrenedione. The regeneration of inhibitor and its potential to inactivate CD45 at substoichiometric (catalytic) concentration was investigated by determining the oxygen dependency of inactivation over an extended incubation time. Shown in Figure 5 are the residual activities of CD45 detected after incubation with a catalytic amount of 2-nitro-9,10-phenanthrenedione in the presence and absence of air. Anaerobic conditions were created by conducting the experiment under argon in oxygen-free buffer (see Materials and Methods for details). In contrast to its negligible inhibition under argon (△), 0.35 μM (0.05 equiv) of the inhibitor mediated a time-dependent and complete inactivation of 7 μM CD45 in the presence of oxygen (▲). The inactivation followed a first-order process with a half-life of ~64 min, which reduced proportionally to a half-life of ~30 min at 0.7 μM inhibitor (●). Thus, CD45 inactivation by 2-nitro-9,10-phenanthrenedione is catalytic and depends on the presence of oxygen.

To probe the reactive species further, the pH dependency of 2-nitro-9,10-phenanthrenedione-catalyzed CD45 inactivation was determined. Between pH 5 and 6, the rates of CD45 inactivation were comparable. However, the rate increased ~25-fold, from 340 (±60) at pH 6.0 to 8400 (±900) M^{-1} s^{-1} at pH 7.5. The markedly accelerated CD45 inactivation correlated well with the ~15-fold enhanced oxygen consumption rate for analogous *o*-quinones from pH 6.0 to 7.5 during redox cycling (*8*, *42*). Catalase (>80 units/mL) or SOD (>10 units/mL) completely protected CD45 over 30 min from inactivation caused by 1.5 μM 2-nitro-9,10-phenanthrenedione under aerobic conditions, further supporting the direct participation of reactive oxygen species derived from quinone-catalyzed redox cycling in its inactivation. Catalase and SOD alone had a negligible effect on CD45 activity.

Specific Oxidation of the Catalytic Cysteine to Sulfenic Acid and Sulfonic Acid. To identify the nature of the chemical modification, PTP1B, after incubation with 1 equiv of 2-nitro-9,10-phenanthrenedione under air at 0 °C, was analyzed by mass spectrometry (Figure 6). The majority of the untreated PTP1B had a molecular mass of 38 718 Da, as expected from its sequence (38 714 Da). A small population was observed at 38 761 Da, consistent with an acetylated PTP1B. After 2 h of incubation with the inhibitor, about half of the protein shifted to a mass of 38 750 Da (Figure 6B; the acetylated population shifted to 38 792 Da), consistent with the addition of two oxygen atoms. The PTP1B was almost completely modified to a new mass of 38 764 Da after 5 h of incubation (Figure 6C), consistent with the addition of three oxygen atoms. To localize the oxidation site, the modified PTP1B after 5 h of incubation was further digested with trypsin and analyzed by LC-MS/MS. Figure 7 shows the MS/MS of its singly charged peptide containing the catalytic cysteine. Compared with that from the unmodified sample (Figure 7A), the pattern of peptide fragment from the modified PTP1B was different as the result of the oxidation. The fragments y8, y9, y16, y17, y18, y20, y21, and b22 (Figure 7B), relative to the unmodified peptide fragmentation (Figure 7A), are 48 Da higher in mass. The fragments y6 through y3, however, remain unmodified. Thus, the catalytic Cys^{215} residue was oxidized to the sulfonic acid ($-SO_3H$). All other cysteine-containing peptides were unmodified under the conditions, demonstrating the specificity of the oxidation. This in turn supports the postulate that the partially oxidized PTP1B after 2 h of incubation corresponds to the catalytic cysteine in the sulfinic state ($-SO_2H$).

DISCUSSION

The data presented here demonstrates that 2-nitro-9,10-phenanthrenedione *catalytically* inactivates CD45 in the presence of DTT in an oxygen-dependent manner. The corresponding PTP1B inactivation was through the specific and sequential oxidation of its catalytic cysteine to the sulfinic acid ($-SO_2H$) and sulfonic acid ($-SO_3H$) via the putative and reversible sulfenic acid ($-SOH$) or its more stable sul-

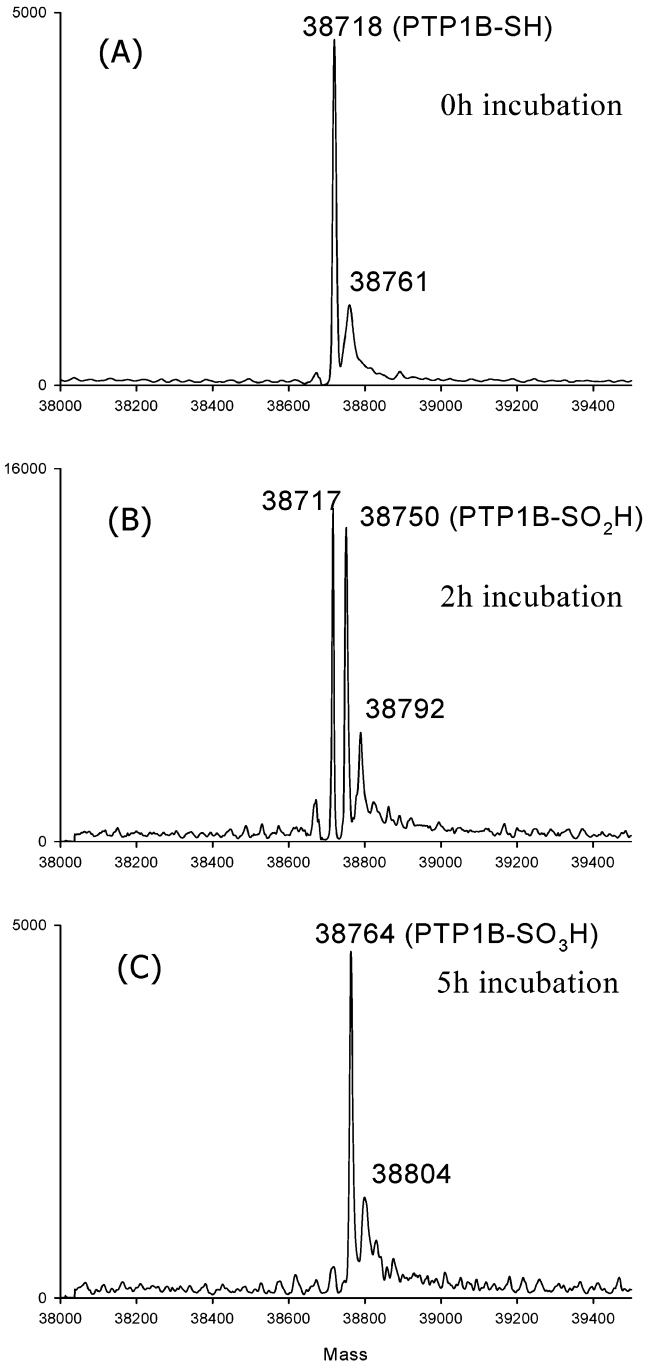

FIGURE 6: Deconvoluted LC-MS spectra of PTP1B after incubation with 2-nitro-9,10-phenanthrenedione at 0 °C under air for (A) 0, (B) 2, or (C) 5 h, expressed as relative intensity versus mass. The expected molecular mass of PTP1B is 38 714 Da, with the peak at 38 761 Da corresponding to an acetylated population (expected at 38 757).

fenyl-amide intermediate. Reactive oxygen species (ROS) and $SQ^{-\bullet}$ radicals derived from quinone-catalyzed redox cycling are involved in the specific cysteine oxidation. The earlier proposal that 9,10-phenanthrenedione-mediated CD45 inhibition was caused by the slow and reversible formation of a thiol-hemiketal intermediate between the catalytic cysteine and quinone was inconsistent with the partial activity recovery reported in Figure 9 of that study (*22*). It is also inconsistent with the lack of a radiolabeled inactive enzyme and the specific oxidation of the catalytic cysteine identified here.

The protein chemistry of quinones is complicated by the coexistence and availability of multiple reaction pathways including addition and redox chemistry. The 1,2-dione functionality of *o*-quinones reacts readily with the guanidinium group of arginine to form a stable adduct in buffer, which remains susceptible to hydrolysis by hydroxylamine (*38*). The chemical feasibility of reversible thiol-hemiketal intermediate formation is supported by the facile carbonyl oxygen scrambling with ^{18}O-water detected by ^{13}C NMR spectroscopy in the present study (see Materials and Methods for details). In addition, *o*- and *p*-quinones react rapidly with protein nucleophiles at their multiple electrophilic sites to form a wide range of stable covalent adducts (*8*, *10*, *43*−*45*). Indeed, covalent adduct formation between an active-site arginine and phenylglyoxal or 1,2-cyclohexanedione was likely responsible for the inhibition of bovine heart PTP (*39*). Thiol conjugation between physiological concentrations of glutathione and 1,4-naphthoquinone derivatives also occurs rapidly under anaerobic conditions (*8*, *46*). Covalent adduct formation between Cdc25 and a biotinylated-1,4-naphthoquinone (*30*) and [^{3}H]vitamin K_3 (2-methyl-1,4-naphthoquinone) (*27*), respectively, supports the notion of thiol-conjugate participation in 1,4-naphthoquinone-mediated Cdc25 inhibition. The lack of enzyme bound radioactivity, derived from [^{125}I]phenanthrenedione-inactivated CD45, eliminated the involvement of any such stable complexes in its inactivation under the present assay conditions. 1,4-Naphthoquinone-mediated CD45 inactivation, at 21 M^{-1} s^{-1}, was mainly mediated by the reactive oxygen species and $SQ^{-\bullet}$ produced during redox cycling, since negligible inhibition was observed under anaerobic conditions at 50 μM inhibitor over 30 min. Thus, it would be interesting to delineate the oxygen-dependent and thiol-conjugate contribution in 1,4-naphthoquinone-mediated Cdc25 inhibition.

Reactive oxygen species including $O_2^{-\bullet}$, H_2O_2, and $SQ^{-\bullet}$ are continuously being generated in the presence of a reducing equivalent (such as DTT), oxygen, and catalytic amounts of quinones that are capable of redox cycling, as illustrated by the scheme in Figure 8 (*8*−*10*). All these reactive species could inactivate PTP. The catalytic cysteine of PTP1B was oxidized to the sulfenic acid (or the sulfenyl-amide) intermediate and subsequently to the sulfinic and sulfonic acids during hydrogen peroxide and superoxide anion radical-mediated inactivation (*13*−*17*). Hydrogen peroxide-mediated inactivation of PTP1B and LAR, at 10−40 $M^{-1}s^{-1}$, was slower than that of 2-nitro-9,10-phenanthrenedione, limiting its contribution. In contrast, the superoxide anion radical-mediated inactivation of PTP1B at 334 M^{-1} s^{-1} (*14*, *15*) was similar to that of 2-nitro-9,10-phenanthrenedione observed here. For superoxide anion radical to contribute significantly to the PTP inactivation, it would have to be accumulated under the present assay conditions. The presence of an initial lag phase in the dose−response of 2-nitro-9,10-phenanthrenedione-catalyzed CD45 inactivation (Figure 2) seems to be consistent with the buildup of such a species. The markedly accelerated PTP inactivation from pH 6 to 7.5 correlated with the high reductant activity of the deprotonated quinol in forming the $SQ^{-\bullet}$ radical, a suspected rate-limiting species in the radical chain propagation of the redox-cycling process (*8*, *10*, *42*). The sensitivities toward catalase and SOD are analogous to their ability to disrupt quinone-catalyzed redox cycling,

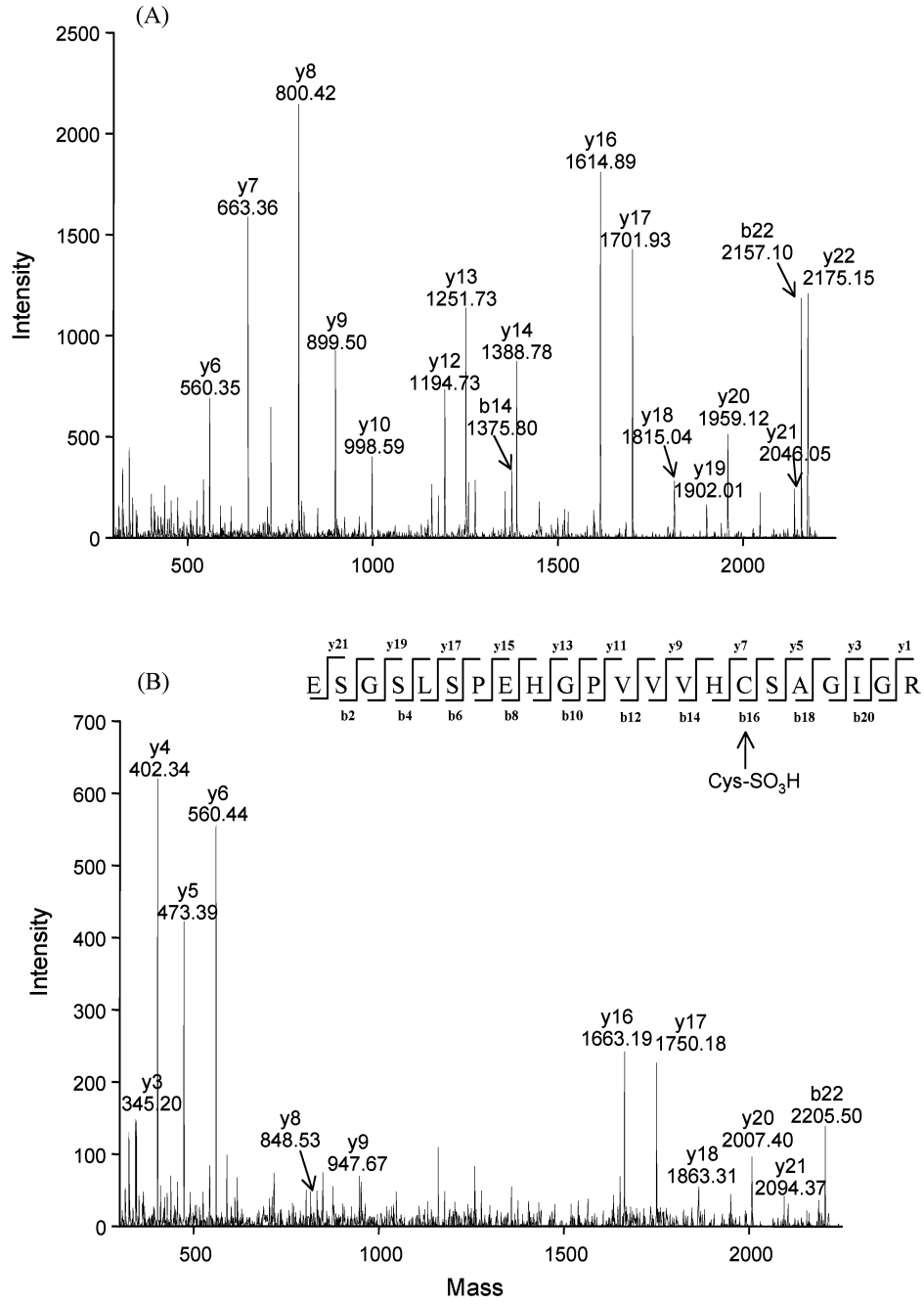

FIGURE 7: LC-MS/MS of the tryptic fragment containing the active-site cysteine (Cys-215) of PTP1B treated with or without 2-nitro-9,-10-phenanthrenedione for 5 h at 0 °C under air.

consistent with the superoxide anion radical participation in chain propagation and PTP inactivation (*42*, *14*, *15*). The ~20-fold enhanced CD45 inactivation by 1,2-naphthoquinone over 1,4-naphthoquinone could be explained by its stronger redox-cycling efficiency (*8*, *10*, *47*). The PTP active site has a strong preference for aryl-containing moieties (*11*, *21*, *31*), which makes the direct participation of the $SQ^{-\bullet}$ radical particularly attractive, thereby resulting in a structure-dependent inhibition of PTPs. Strong $SQ^{-\bullet}$ radical signals have been observed by electron spin resonance spectroscopy after mixing of glutathione with benzoquinone or naphthoquinone in HEPES buffers at room temperature (*48*, *49*), suggesting a sustained and abundant flux of $SQ^{-\bullet}$ radical during redox cycling (*8*). The preferential and selective binding of a $SQ^{-\bullet}$ radical with the PTP active site could lead to an efficient and structure-dependent production of the catalytic cysteine radical, which subsequently terminates directly or indirectly to the reversible sulfenic acid or a disulfide species as the initial product. Further oxidation of these species would lead to the irreversible and sequential formation of the sulfinic acid and sulfonic acid. This may provide an explanation for the structure-dependent and differential inhibition of CD45 and PTP1B among the 9,-10-phenanthrenedione derivatives (*22*).

Among the diverse bioresponses, the long-term mutagenic effects of quinones are best understood. Many quinones are planar in structure, intercalate effectively between the DNA base pairs, and act as chemical nucleases by harvesting and propagating surrounding free radicals, with their abundance further augmented by the redox-cycling process (*8*−*10*). The

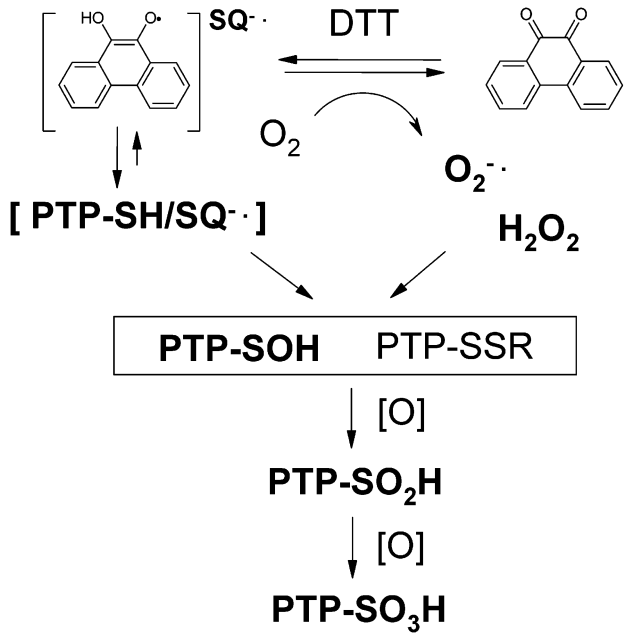

FIGURE 8: Proposed scheme for the catalytic inactivation of PTP by quinones from redox cycling. 9,10-Phenanthrenedione is reduced by DTT to a semiquinone anion radical ($SQ^{-\bullet}$), which reduces oxygen to superoxide anion radical ($O_2^{-\bullet}$) and re-forms the quinone. Both $SQ^{-\bullet}$ and $O_2^{-\bullet}$ radicals could contribute to the specific oxidation of the catalytic cysteine, via a transient (PTP−SH/$SQ^{-\bullet}$) intermediate for $SQ^{-\bullet}$. PTP−SH, PTP−SOH, PTP−SO_2H, and PTP−SO_3H represent the thiol and sulfenic, sulfinic, and sulfonic acid states of the catalytic nucleophile. PTP−SSR represents a putative disulfide adduct with DTT. PTP−SOH and PTP−SSR would be sensitive to hydroxylamine- and DTT-mediated reactivation.

mechanisms behind their acute cellular responses can be largely attributed to their redox cycling. In the presence of oxygen, *o*-quinones, generally more reactive than *p*-quinones, catalyze the continuous oxidation of glutathione, ascorbate, NAD(P)H, and dihydrolipoamide to generate ROS and $SQ^{-\bullet}$, thereby altering the cellular redox state and the activities of thiol-enzymes including PTPs. Contrary to their less-selective chemical reactivity, some quinones elicit limited and specific cellular responses, signifying the presence of selective targeting. Their aryl-structural feature not only dictates their redox potential and redox-cycling efficiency but also may guide them selectively toward the aryl-preferring PTPs and other preferred targets in the cellular protein milieu. The potential participation of the semiquinone radical in PTP inactivation opens the possibility of designing selective quinones for therapeutic usage.

In summary, many quinones are catalytic inactivators of protein tyrosine phosphatases under aerobic conditions, through the specific oxidation of their catalytic cysteine. In addition to serving as vital links in electron transport, naturally occurring quinones may act as efficient regulators of protein tyrosine phosphorylation in biological systems. Aberrant phosphotyrosine homeostasis resulting from continued polyaromatic hydrocarbon quinone exposure may play a significant role in their disease etiology.

ACKNOWLEDGMENT

We thank Deena Waddelton, Marc Oullet, Jean-Pierre Falgueyret, Brian Kennedy, Ernest Asante-Appiah, and Dave Percival for many helpful discussions.

REFERENCES

1. Bindoli, A., Rigobello, M. P., and Deeble, D. J. (1992) Biochemical and toxicological properties of the oxidation products of catecholamines, *Free Radical Biol. Med. 13*, 391−405.
2. Phillips D. H. (1999) Polycyclic aromatic hydrocarbons in the diet, *Mutat. Res. 443*, 139−147.
3. Peltonen K., and Dipple, A. (1995) Polycyclic aromatic hydrocarbons: Chemistry of DNA adduct formation, *J. Occup. Environ. Med. 37*, 52−58.
4. Ward, E. C., Murray, M. J., Lauer, L. D., House, R. V., and Dean, J. H. (1986) Persistent suppression of humoral and cell-mediated immunity in mice following exposure to the polycyclic aromatic hydrocarbon 7,12-dimethylbenz[*a*]anthracene, *Int. J. Immunopharmacol. 8*, 13−22.
5. Lee, K. H. (1999) Novel antitumor agents from higher plants, *Med. Res. Rev. 19*, 569−596.
6. Workman, P. (1994) Enzyme-directed bioreductive drug development revisited: a commentary on recent progress and future prospects with emphasis on quinone anticancer agents and quinone metabolizing enzymes, particularly DT-diaphorase, *Oncol. Res. 6*, 461−475.
7. Koster, A. S. (1991) Bioreductive activation of quinones: a mixed blessing, *Pharm. Weekbl. Sci. 13*, 123−126.
8. O'Brien, P. J. (1991) Molecular mechanisms of quinone cytotoxicity, *Chem.-Biol. Interact. 80*, 1−41.
9. Wardman, P. (1990) Bioreductive activation of quinones: redox properties and thiol reactivity, *Free Radical Res. Commun. 8*, 219−229.
10. Brunmark, A., and Cadenas, E. (1989) Redox and addition chemistry of quinoid compounds and its biological implications, *Free Radical Biol. Med. 7*, 435−477.
11. Wang, W. Q., Sun, J. P., and Zhang, Z. Y. (2003) An overview of the protein tyrosine phosphatase superfamily, *Curr. Top Med. Chem. 3*, 739−748.
12. Tonks, N. K. (2003) PTP1B: from the sidelines to the front lines! *FEBS Lett. 546*, 140−148.
13. Denu, J. M., and Tanner, K. G. (1998) Specific and reversible inactivation of protein tyrosine phosphatases by hydrogen peroxide: evidence for a sulfenic acid intermediate and implications for redox regulation, *Biochemistry 37*, 5633−5642.
14. Barrett, W. C., DeGnore, J. P, Keng, Y. F., Zhang, Z. Y., Yim, M. B., and Chock, P. B. (1999) Roles of superoxide radical anion in signal transduction mediated by reversible regulation of protein-tyrosine phosphatase 1B, *J. Biol. Chem. 274*, 34543−34546.
15. Barrett, W. C., DeGnore, J. P., Konig, S., Fales, H. M., Keng, Y. F., Zhang, Z. Y., Yim, M. B., and Chock, P. B. (1999) Regulation of PTP1B via glutathionylation of the active site cysteine 215, *Biochemistry 38*, 6699−6705.
16. van Montfort, R. L., Congreve, M., Tisi, D., Carr, R., and Jhoti, H. (2003) Oxidation state of the active-site cysteine in protein tyrosine phosphatase 1B, *Nature 423*, 773−777.
17. Salmeen, A., Andersen, J. N., Myers, M. P., Meng, T. C., Hinks, J. A., Tonks, N. K., and Barford D. (2003) Redox regulation of protein tyrosine phosphatase 1B involves a sulphenyl-amide intermediate, *Nature 423*, 769−773.
18. Zhang, Z. Y., and Lee, S. Y. (2003) PTP1B inhibitors as potential therapeutics in the treatment of type 2 diabetes and obesity, *Expert Opin. Investig. Drugs. 12*, 223−233.
19. Irie-Sasaki, J., Sasaki, T., and Penninger, J. M. (2003) CD45 regulated signaling pathways, *Curr. Top Med. Chem. 3*, 783−796.
20. Ramachandran, C., and Kennedy, B. P. (2003) Protein tyrosine phosphatase 1B: a novel target for type 2 diabetes and obesity, *Curr. Top Med. Chem. 3*, 749−757.
21. Taylor, S. D. (2003) Inhibitors of protein tyrosine phosphatase 1B (PTP1B), *Curr. Top Med. Chem. 3*, 759−782.
22. Urbanek, R. A., Suchard, S. J., Steelman, G. B., Knappenberger, K. S., Sygowski, L. A., Veale, C. A., and Chapdelaine, M. J. (2001) Potent reversible inhibitors of the protein tyrosine phosphatase CD45, *J. Med. Chem. 44*, 1777−1793.
23. Lazo, J. S., Nemoto, K., Pestell, K. E, Cooley, K., Southwick, E. C., Mitchell, D. A., Furey, W., Gussio, R., Zaharevitz, D. W., Joo, B., and Wipf, P. (2002) Identification of a potent and selective pharmacophore for Cdc25 dual specificity phosphatase inhibitors, *Mol. Pharmacol. 61*, 720−728.
24. Ahn, J. H., Cho, S. Y., Ha, J. D., Chu, S. Y., Jung, S. H., Jung, Y. S., Baek, J. Y., Choi, I. K., Shin, E. Y., Kang, S. K., Kim, S. S., Cheon, H. G., Yang, S. D., and Choi, J. K. (2002) Synthesis

and PTP1B inhibition of 1,2-naphthoquinone derivatives as potent anti-diabetic agents, *Bioorg. Med. Chem. Lett. 12*, 1941−1946.
25. Carr, B. I., Wang, Z., and Kar, S. (2002) K vitamins, PTP antagonism, and cell growth arrest, *J. Cell Physiol. 193*, 263−274.
26. Ni, R., Nishikawa, Y., and Carr, B. I. (1998) Cell growth inhibition by a novel vitamin K is associated with induction of protein tyrosine phosphorylation, *J. Biol. Chem. 273*, 9906−9911.
27. Wu, F. Y., and Sun, T. P. (1999) Vitamin K3 induces cell cycle arrest and cell death by inhibiting Cdc25 phosphatase, *Eur. J. Cancer 35*, 1388−1393.
28. Ham, S. W., Park, J., Lee, S. J., and Yoo, J. S. (1999) Selective inactivation of protein tyrosine phosphatase PTP1B by sulfone analogue of naphthoquinone, *Bioorg. Med. Chem. Lett. 18*, 185−186.
29. Nishikawa, Y., Wang, Z., Kerns, J., Wilcox, C. S., and Carr, B. I. (1999) Inhibition of hepatoma cell growth in vitro by arylating and nonarylating K vitamin analogues. Significance of protein tyrosine phosphatase inhibition, *J. Biol. Chem. 274*, 34803−34810.
30. Kar, S., Lefterov, I. M., Wang, M., Lazo, J. S., Scott, C. N., Wilcox, C. S., and Carr, B. I. (2003) Binding and inhibition of Cdc25 phosphatases by vitamin K analogues, *Biochemistry 42*, 10490−10497.
31. Huang, Z., Wang, Q. P., Abdullah, K., Dube, D., Friesen, R., Trimble, L., Gorvindarajin, A., Sanghara, C., Li, C., and Ramachandran, C. (2001) Catalytic inactivation of protein tyrosine phosphatases CD45 and PTP 1B by polyaromatic *ortho*-quinones, 84th CSC Conference and Exhibition, Montreal, Quebec, May 20−30, 2001.
32. Novikov, A. N., Slyusarchuk, V. T., and Matantseva, E. F. (1977) Synthesis of iodo derivatives of phenanthrenequinone and diphenic acid, *Izv. Tomsk. Politekhn. Inst. 214*, 72−74 [*Chem. Abstr*. (1978) *214*, 24025a].
33. Mega, T. L., and Van Etten, R. L. (1990) Oxygen exchange and bond cleavage reactions of carbohydrates studied using the ^{18}O isotope shift in ^{13}C NMR spectroscopy, *Basic Life Sci. 56*, 85−93.
34. Huang, Z., Wang, Q. P., Hoa, D. L., Gorvindarajan, A., Scheigetz, J., Zamboni, R., Desmarais, S., and Ramachandran, C. (1999) 3,6-Fluorescein Diphosphate: A Sensitive Fluorogenic and Chromogenic Substrate for Protein Tyrosine Phosphatases, *J. Biomol. Screening 4*, 327−334.
35. Huyer, G., Liu, S., Kelly, J., Moffat, J., Payette, P., Kennedy, B., Tsaprailis, G., Gresser, M. J., and Ramachandran, C. (1997) Mechanism of inhibition of protein-tyrosine phosphatases by vanadate and pervanadate, *J. Biol. Chem. 272*, 843−851.
36. Ellis, H. R., and Poole, L. B. (1997) Novel application of 7-chloro-4-nitrobenzo-2-oxa-1,3-diazole to identify cysteine sulfenic acid in the AhpC component of alkyl hydroperoxide reductase, *Biochemistry 36*, 15013−15018.
37. Desmarais, S., Friesen, R. W., Zamboni, R., and Ramachandran, C. (1999) Difluro(phosphono)methyl]phenylalanine-containing peptide inhibitors of protein tyrosine phosphatases, *Biochem. J. 337*, 219−223.
38. Patthy, L., and Smith, E. L. (1975) Reversible modification of arginine residues. Application to sequence studies by restriction of tryptic hydrolysis to lysine residues, *J. Biol. Chem. 250*, 557−564.
39. Zhang, Z. Y., Davis, J. P., Van Etten, R. L. (1992) Covalent modification and active site-directed inactivation of a low molecular weight phosphotyrosyl protein phosphatase, *Biochemistry 31*, 1701−1711.
40. Claiborne, A., Yeh, J. I., Mallett, T. C., Luba, J., Crane, E. J., 3rd, Charrier, V., and Parsonage, D. (1999) Protein-sulfenic acids: diverse roles for an unlikely player in enzyme catalysis and redox regulation, *Biochemistry 38*, 15407−15416.
41. Allision, W. S. (1976) Formation and reactions of sulfenic acids in proteins, *Acc. Chem. Res. 9*, 293−299.
42. Molina Portela, M. P., and Stoppani, A. O. (1996) Redox cycling of beta-lapachone and related *o*-naphthoquinones in the presence of dihydrolipoamide and oxygen, *Biochem Pharmacol. 51*, 275−283.
43. Finley, K. T. (1988) Quinones as synthones, in *The chemistry of the quinoid compounds* (Patai, S., and Rappoport, Z., Eds.) Chapter 11, pp 537−717, John Wiley & Sons Ltd., New York.
44. Murty, V. S., and Penning, T. M. (1992) Polycyclic aromatic hydrocarbon (PAH) ortho-quinone conjugate chemistry: kinetics of thiol addition to PAH ortho-quinones and structures of thioether adducts of naphthalene-1,2-dione, *Chem.-Biol. Interact. 84*, 169−188.
45. Buffinton, G. D., Ollinger, K., Brunmark, A., and Cadenas, E. (1989) DT-diaphorase-catalysed reduction of 1,4-naphthoquinone derivatives and glutathionyl-quinone conjugates. Effect of substituents on autoxidation rates, *Biochem. J. 257*, 561−571.
46. Wilson, I., Wardman, P., Lin, T. S., and Sartorlli, A. C. (1987) Reactivity of thiols towards derivatives of 2- and 6-methyl-1,4-naphthoquinone bioreductive alkylating agents, *Chem.-Biol. Interact. 61*, 229−240.
47. Roginsky, V. A., Barsukova, T. K., and Stegmann, H. B. (1999) Kinetics of redox interaction between substituted quinones and ascorbate under aerobic conditions, *Chem.-Biol. Interact. 121*, 177−197.
48. Gant, T. W., Doherty, M., Odowole, D., Sales, K. D., and Cohen, G. M. (1986) Semiquinone anion radicals formed by the reaction of quinones with glutathione or amino acids, *FEBS Lett. 201*, 296−300.
49. Rao, D. N. R., Takahashi, N., and Mason, R. P. (1988) Characterization of a glutathione conjugate of the 1,4-benzosemiquinone-free radical formed in rat hepatocytes, *J. Biol. Chem. 263*, 17981−17986.

BI035986E